Thermodynamic Properties of $[C_6mim][NTf_2]$ in the Condensed State

Andrey V. Blokhin, Yauheni U. Paulechka, and Gennady J. Kabo*

Belarusian State University, Chemistry Faculty, Leningradskaya 14, 220030 Minsk, Belarus

Heat capacities of 1-hexyl-3-methylimidazolium bis(trifluoromethylsulfonyl)imide $[C_6mim][NTf_2]$ have been measured with a new adiabatic calorimeter in a range of temperatures of (5 to 370) K. The substance was found to form glass with $T_g = 184.3$ K and $\Delta^l_{gl}C_{s,m} = (170.7 \pm 2.8)$ J·K^{-1}·mol^{-1}. At different modes of crystallization $[C_6mim][NTf_2]$ forms at least three crystals, the heat capacities of which differ up to 2 % in the temperature range of (220 to 250) K but coincide within 0.1 % in the temperature range of (80 to 220) K. Triple-point temperature for all the crystals is $T_0 = (272.03 \pm 0.01)$ K, but the enthalpies of fusion are somewhat different. Thermodynamic properties for $[C_6mim][NTf_2]$ are calculated based on the obtained data.

Introduction

Recently a number of publications dealing with properties of room temperature ionic liquids (IL) has been growing exponentially because of unique properties of ILs for chemistry and chemical technology.[1] Earlier we found that ability of 1-alkyl-3-methylimidazolium bromides to crystallize and vitrify strongly depend on the length of the alkyl chain.[2] An anomaly was reported for $[C_2mim]Br$ at $T = 13$ K.[2] Specific heat capacity for $[C_4mim][PF_6]$ in the range of $T < 30$ K should also be considered as anomalously high as compared with most molecular organic crystals.[3] During heat capacity measurements for $[C_6mim][NTf_2]$ in the condensed state, it was found that this compound forms different crystal phases in a range of temperatures of (220 to 260) K.

According to IACT/IUPAC Project 2002-005-1-100, $[C_6mim][NTf_2]$ is assumed to be a reference compound for physicochemical properties of ILs.[4] Therefore, in this work particular attention has been given to calibration and checking of an adiabatic calorimeter.

Experimental Section

A sample of $[C_6mim][NTf_2]$ was synthesized by Dr. Mark Muldoon from the University of Notre Dame. Purity of the sample was determined from ^1H and ^{19}F spectroscopy to be > 99.5 %. Water content of 5 ppm was found by the Fisher titration.

Heat capacities in the condensed state in a range of temperatures from (5 to 370) K and enthalpy of fusion for $[C_6mim][NTf_2]$ were measured in a TAU-10 vacuum adiabatic calorimeter (Termis, Moscow).[5,6] A scheme of the calorimetric unit of the calorimeter is presented in Figure 1.

A sample was loaded into a container. The container was a thin-walled titanium cylinder with internal volume of ≈ 1 cm^3. A titanium cap of the container was sealed with an indium O-ring and fixed with a brass gasket. The container was exposed to vacuum of ≈ 3 Pa for 0.5 h and then filled with helium gas to the pressure of 5 kPa at 290 K. The container was slid into a heating tube suspended with nylon threads inside a copper adiabatic shield. The heater was made of 0.06 mm manganin wire wound on the tube and coated with 0.03 mm copper foil. Temperature was measured with a Fe/Rh resistance thermometer ($R_0 = 50$ Ω) calibrated on ITS-90 by VNIIFTRI (Moscow). The thermometer was located on an inner surface of the adiabatic shield. The temperature difference between the tube and the shield was measured with a differential thermocouple (Cu + 0.1 % Fe)/chromel. Eleven junctions of the thermocouple are sited on the copper foil of the heating tube, and the other 12 are sited on the lower part of the inner surface of the shield.

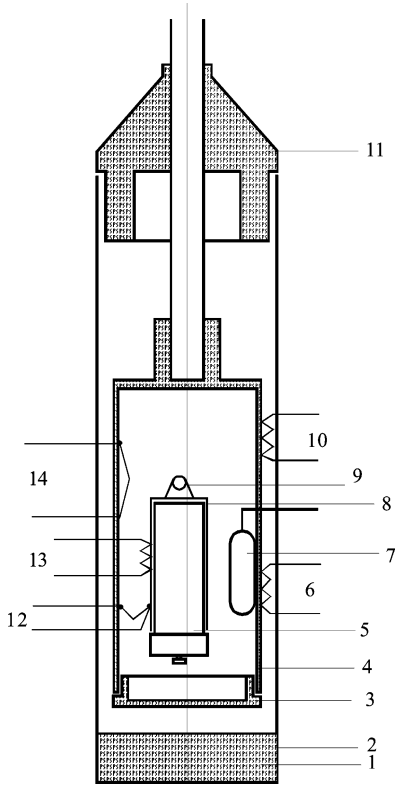

Figure 1. Scheme of a TAU-10 calorimeter: 1, charcoal getter; 2, vacuum jacket; 3, removable shield lid; 4, adiabatic shield; 5, sample container; 6, main heater of the adiabatic shield; 7, Fe/Rh resistance thermometer; 8, heating tube; 9, nylon threads; 10, gradient heater of the adiabatic shield; 11, copper plug (vacuum tight); 12, 11−12-junction differential thermocouple (Cu + 0.1 % Fe)/chromel; 13, heater of the tube; 14, gradient 3−4-junction differential thermocouple (Cu + 0.1 % Fe)/chromel.

* Corresponding author. Fax: +375-17-2203-916; E-mail: shevelyova_marina@yahoo.com or kabo@bsu.by.

10.1021/je060094d CCC: $33.50
Published on Web 06/29/2006

Table 1. Sample Masses (m_s) Used in Calorimetric Measurements and Contributions of Sample Heat Capacity to the Measured Total (Sample + Cell) Heat Capacity [$(C_{p,sample}/C_{sum})\cdot 100$] % at Selected Temperatures

	m_s	[$(C_{p,sample}/C_{sum})\cdot 100$] %			
compound	g	$T \approx 10$ K	$T \approx 50$ K	$T \approx 100$ K	$T \approx 300$ K
corundum	1.9042			24	52
copper	7.6144	46	71	71	68
benzoic acid	0.8689[a]			36	43
	0.8060[b]	70	49		
[C_6mim][NTf_2]	1.1769[c]	84	55	44	55
	0.6579[d]			31	40

[a] Measurements in the temperature range (80 to 370) K (series 1 and 2, Table S3). [b] Measurements in the temperature range (5 to 78) K (series 3, Table S3). [c] Measurements in the temperature range (5 to 370) K (series 1 to 11, Table 2). [d] Measurements in the temperature range (80 to 370) K (series 12 to 25, Table 2).

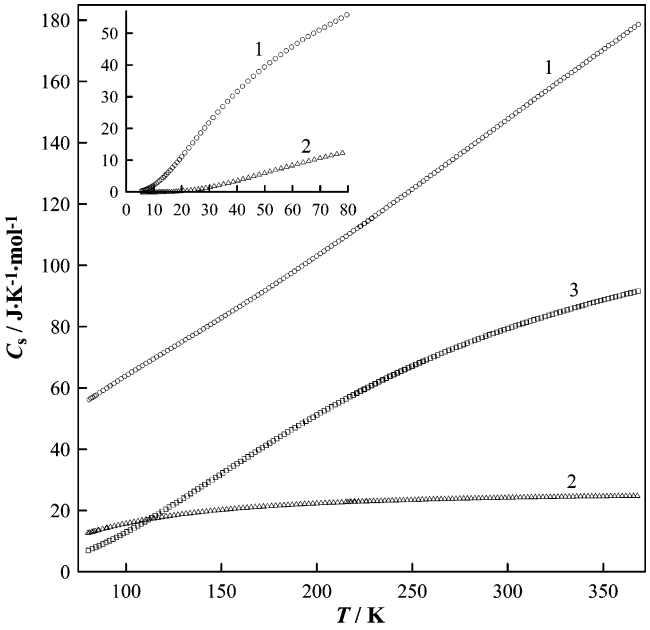

Figure 2. Experimental heat capacities of selected reference materials: 1, benzoic acid; 2, copper; 3, corundum (α-Al_2O_3).

Adiabatic conditions are maintained to within $\pm \leq (1\cdot 10^{-3})$ K with the software applying proportional integral temperature adjustment.

Thermal anchors for electric wires were placed on the top of the shield. When the temperature difference between the shield and a cooling bath was high, these wires (together with a tube carrying the shield) cause a temperature gradient along the shield. This may lead to additional errors in measurements. To control this gradient, an additional 3−4-junction thermocouple between the middle and the upper parts of the shield was applied. The temperature gradient was adjusted to zero with an additional gradient heater.

To control the calorimeter and acquire the data, an AK-6.25 device[7] was used. A "Heat" software program[6] was applied for interaction of the device with a computer. Two modes of heat capacity measurements were possible: a constant-temperature mode and a constant-heat mode. Both the modes can be applied in measurements of normal heat capacity of a sample, but in the phase-transition range where low-temperature increments correspond to high heat inputs the second mode was used.

Heating periods of calorimetric experiments for determination of normal heat capacity were of (60 to 150) s at $T =$ (5 to 40) K, (200 to 250) s at $T =$ (40 to 80) K, and 400 s at $T >$ 80 K. Thermal relaxation time was within (80 to 160) s at $T <$ 80 K

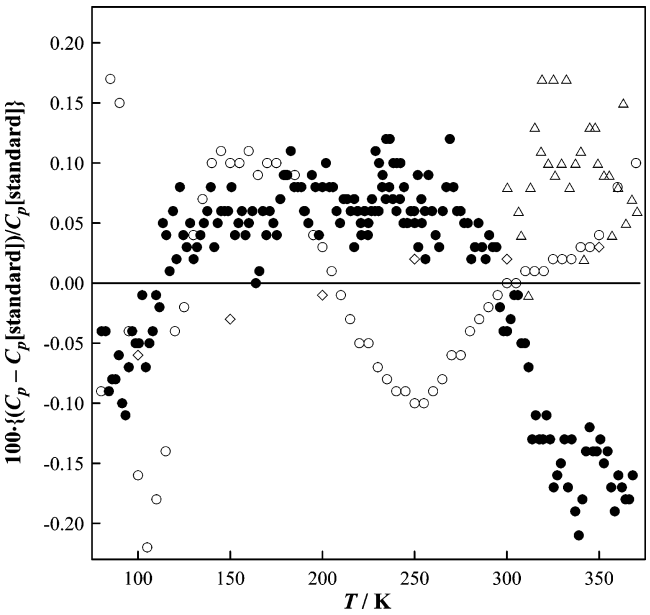

Figure 3. Percentage deviations of the heat capacities (C_p) of corundum from the standard values (C_p[standard]) recommended by Ditmars et al.:[11] ●, this work; ○, recommended by Furukawa et al.;[12] △, Andrews et al.;[13] ◇, recommended by Sabbah et al.[8]

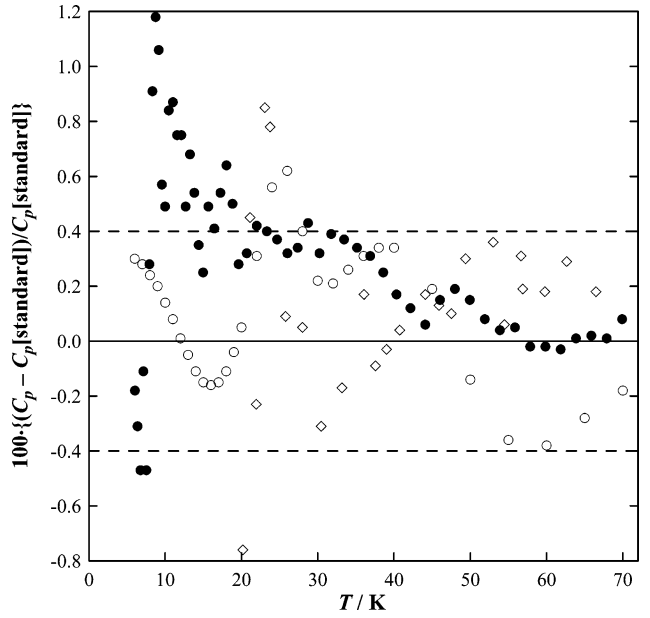

Figure 4. Percentage deviations of the heat capacities (C_p) of copper in the temperature range of (6 to 70) K from the standard values (C_p[standard]) recommended by Sabbah et al.:[8] ●, this work; ○, recommended by White and Collocott;[9] ◇, Stevens and Boerio-Coates.[14]

and ≥ 200 s over the remaining temperature range. The periods for drift measurement were (200 to 250) s at $T <$ 80 K and ≥ 300 s at $T >$ 80 K. A temperature step of the measurements was ≥ 1/10T at $T <$ 40 K and ≥ 2.5 K at $T >$ 40 K.

The reliability of the calorimeter was checked in measurements for reference corundum (VNIIM, St.-Petersburg, Russia) in a range of temperatures (80 to 370) K, high-purity copper (mass fraction ≥ 0.99995) in a range of temperatures (6 to 370) K, and benzoic acid (K-1 grade, mass fraction ≥ 0.99995) in a range of temperatures of (5 to 370) K. These substances were recommended as reference materials for adiabatic calorimetry by Sabbah et al.[8] in the temperature ranges of (10 to 500) K, (1 to 300) K, and (10 to 350) K, respectively. Masses of the samples and ratios C_p(sample)/C_p(sample + cell) at several

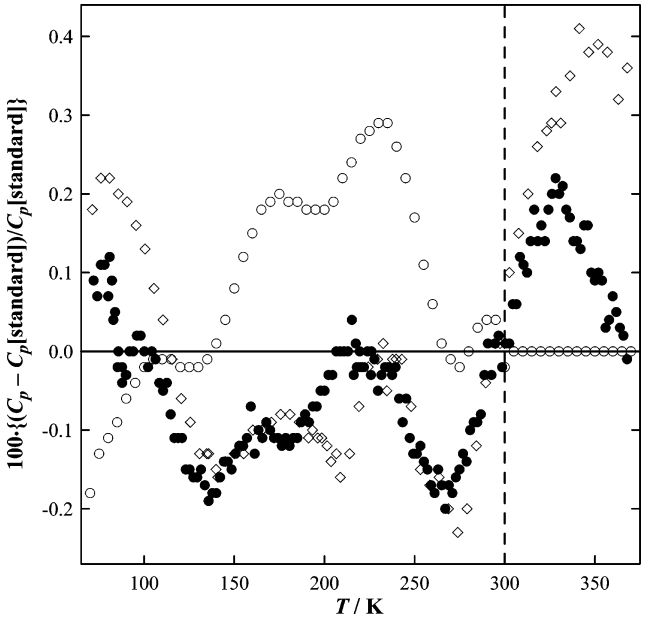

Figure 5. Percentage deviations of the heat capacities (C_p) of copper in the temperature range of (70 to 370) K from the standard values (C_p[standard]) recommended by Sabbah et al.[8] for the temperature range (70 to 300) K and by White and Collocott[9] for the temperature range (300 to 370) K: ●, this work; ○, recommended by White and Collocott;[9] ◇, Stevens and Boerio-Coates.[14]

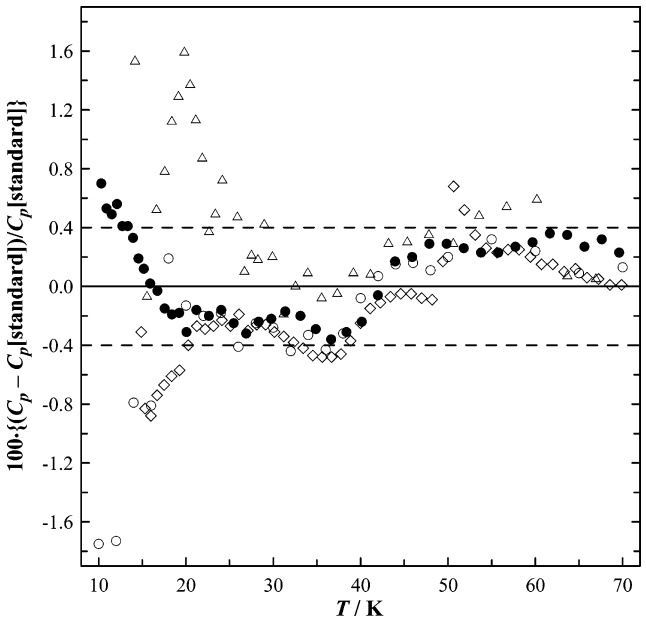

Figure 6. Percentage deviations of the heat capacities (C_p) of benzoic acid in the temperature range (10 to 70) K from the standard values (C_p[standard]) recommended by Sabbah et al.:[8] ●, this work; ○, recommended by Rybkin et al.;[10] ◇, Kobashi et al.;[15] △, Tatsumi et al.[16]

temperatures are presented in Table 1. Experimental heat capacities of corundum, copper, and benzoic acid are shown in Tables S1 to S3 (in the Supporting Information) and in Figure 2. The rms deviations of experimental points from the smoothing polynomial curves do not exceed 0.1 % at $T > 20$ K and 0.3 % at lower temperatures.

Our results are compared with the literature values in Figures 3 to 7. The obtained results allow us to assume that relative error in heat capacity measurements with the calorimeter does not exceed ± 0.4 % in the main temperature range of (20 to 370) K and ± 1 % in the range of (10 to 20) K. Heat capacities of copper obtained in this work in the interval (6 to 10) K differ

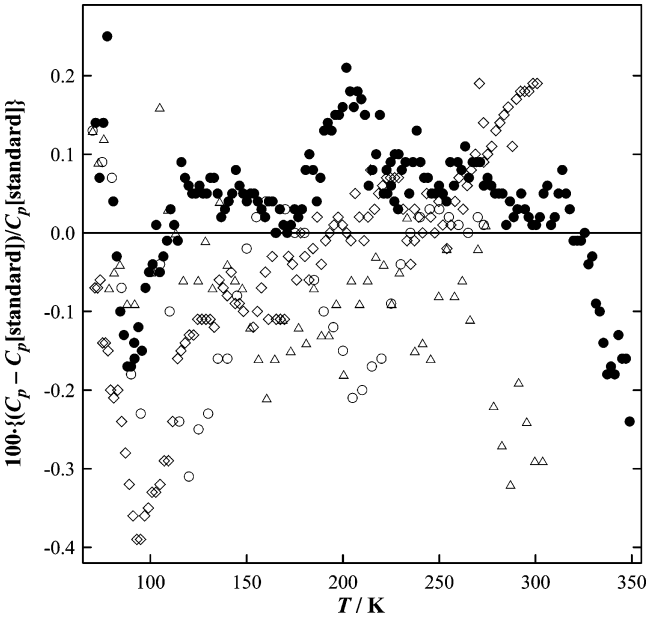

Figure 7. Percentage deviations of the heat capacities (C_p) of benzoic acid in the temperature range (70 to 350) K from the standard values (C_p[standard]) recommended by Sabbah et al.:[8] ●, this work; ○, recommended by Rybkin et al.;[10] ◇, Kobashi et al.;[15] △, Tatsumi et al.[16]

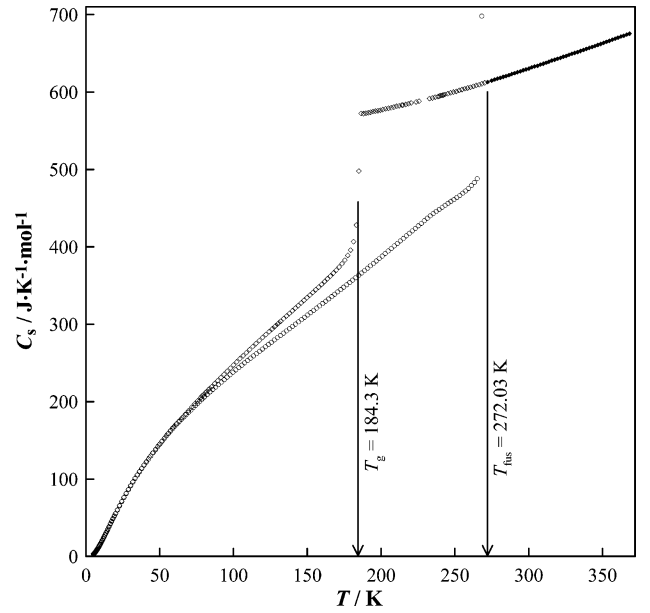

Figure 8. Experimental heat capacities of $[C_6mim][NTf_2]$ in the glassy, crystal and liquid states at vapor-saturation pressure: ◇, glass and supercooled liquid (at $T < T_{fus}$); ◆, liquid (at $T > T_{fus}$); ○, crystal β (series 4 and 10); T_g is the glass transition temperature; T_{fus} is the triple point temperature.

from those recommended by Sabbah et al.[8] and White and Collocott[9] by < 1.2 %. The experimental values of C_p for benzoic acid in the temperature range of (5 to 10) K agree with those recommended by Rubkin et al.[10] within 2 %. Hence we conclude that the relative uncertainty of heat capacity measurements in the calorimeter does not exceed ± 2 % at $T < 10$ K.

Results and Discussion

Experimental heat capacities for $[C_6mim][NTf_2]$ in the condensed state in the range of temperatures of (5 to 370) K are given in Table 2 and in Figure 8. In Figure 8, heat capacities for the crystal are represented by the values for the β crystal from series 4 and 10. Two samples were used in the measure-

Table 2. Experimental Molar Heat Capacities of [C_6mim][NTf_2] in the Condensed State at Vapor-Saturation Pressure (R = 8.314472 J·K^{-1}·mol^{-1})

⟨T⟩	$C_{s,m}$[a]	⟨T⟩	$C_{s,m}$[a]	⟨T⟩	$C_{s,m}$[a]	⟨T⟩	$C_{s,m}$[a]	⟨T⟩	$C_{s,m}$[a]	⟨T⟩	$C_{s,m}$[a]	⟨T⟩	$C_{s,m}$[a]
K	R	K	R	K	R	K	R	K	R	K	R	K	R
series 1		261.29	57.57	152.23	37.87	294.50	75.39	252.84	72.41	54.55	18.73	67.335	22.09
glass		263.39	58.14	154.28	38.22	296.43	75.57	254.76	72.54	55.98	19.09	69.521	22.64
78.73	24.95	265.47	58.87	156.32	38.58	298.37	75.72	256.68	72.68	57.39	19.47	71.671	23.19
80.97	25.44	267.50	62.74	158.35	38.93	series 5		258.60	72.80	58.81	19.85	73.717	23.71
83.05	25.91	269.24	93.54	160.39	39.30	supercooled liquid		series 7		60.24	20.23	75.691	24.15
85.15	26.37	liquid		162.43	39.65	250.85	72.26	supercooled liquid		61.70	20.59	77.697	24.66
87.25	26.85	273.07	77.50	164.46	40.02	252.87	72.40	232.78	71.13	63.19	20.92	79.750	25.14
89.37	27.33	274.91	73.94	166.50	40.37	254.79	72.55	234.71	71.24	64.74	21.30	81.810	25.61
91.49	27.81	276.78	74.08	168.53	40.74	256.71	72.66	236.56	71.36	66.33	21.66	83.863	26.09
93.63	28.30	series 3		170.56	41.10	258.63	72.78	238.40	71.46	67.96	22.03	series 12	
95.78	28.78	crystal β		172.58	41.47	260.55	72.91	240.25	71.60	69.60	22.39	supercooled liquid	
97.93	29.27	201.65	46.83	174.61	41.83	262.48	73.05	242.09	71.70	71.20	22.75	194.39	69.11
100.09	29.75	203.97	47.27	176.64	42.20	264.40	73.19	series 8		72.74	23.12	196.16	69.21
102.25	30.23	206.28	47.72	178.66	42.55	266.32	73.29	supercooled liquid		74.22	23.45	197.85	69.30
104.42	30.72	208.59	48.16	180.68	42.93	268.25	73.45	223.68	70.61	75.68	23.77	199.54	69.38
106.60	31.19	210.89	48.60	182.69	43.30	270.17	73.58	225.60	70.73	77.19	24.10	201.23	69.46
108.78	31.67	213.18	49.04	184.71	43.67	liquid		series 9		78.72	24.45	202.93	69.57
110.97	32.13	215.48	49.49	186.72	44.04	272.10	73.70	supercooled liquid		80.25	24.77	204.63	69.64
113.16	32.61	217.77	49.94	188.73	44.41	274.84	73.93	214.71	70.12	82.03	25.14	206.33	69.79
115.36	33.08	220.06	50.39	190.73	44.78	276.85	74.09	216.63	70.23	84.08	25.58	208.03	69.97
117.55	33.55	222.33	50.81	192.73	45.15	278.78	74.23	218.45	70.34	series 11		series 13	
119.75	34.01	224.61	51.25	194.73	45.52	280.71	74.35	220.28	70.46	glass		crystal γ, partly	
121.95	34.48	226.88	51.70	196.73	45.91	282.65	74.50	series 10		5.165	0.4358	amorphous	
124.15	34.92	229.15	52.13	198.72	46.29	284.58	74.64	crystal β		5.397	0.4945	78.42	24.31
126.36	35.38	231.41	52.59	200.71	46.66	286.52	74.78	5.101	0.3013	5.712	0.5762	80.58	24.73
128.56	35.85	233.66	52.99	202.73	47.07	288.45	74.95	5.301	0.3456	6.034	0.6643	82.51	25.11
130.76	36.30	235.91	53.36	204.79	47.46	290.39	75.08	5.506	0.3948	6.399	0.7644	84.43	25.52
series 2		238.15	53.75	206.85	47.84	292.32	75.23	5.715	0.4459	6.801	0.8869	86.36	25.89
glass		240.39	54.11	208.90	48.26	294.26	75.37	5.929	0.4984	7.204	1.021	88.29	26.29
125.90	35.28	242.63	54.47	210.95	48.63	296.20	75.54	6.173	0.5633	7.609	1.155	90.23	26.70
128.01	35.71	244.86	54.82	213.00	49.02	298.14	75.66	6.346	0.6124	8.018	1.299	92.16	27.09
129.99	36.12	247.09	55.16	215.04	49.41	300.08	75.79	6.637	0.6989	8.429	1.451	94.10	27.47
131.98	36.54	249.32	55.48	217.08	49.81	302.02	76.00	7.032	0.8290	8.841	1.608	96.05	27.85
133.96	36.95	251.54	55.81	219.11	50.20	303.96	76.13	7.429	0.9607	9.254	1.770	98.00	28.23
135.94	37.35	253.84	56.15	221.14	50.58	305.90	76.23	7.829	1.104	9.668	1.937	99.94	28.61
137.93	37.76	256.16	56.56	223.18	50.96	307.84	76.41	8.233	1.255	10.083	2.106	101.90	28.96
139.91	38.17	258.38	57.04	225.20	51.36	309.78	76.55	8.638	1.412	10.607	2.329	103.85	29.34
141.89	38.57	series 4		227.23	51.75	311.72	76.71	9.045	1.577	11.242	2.603	105.81	29.71
143.87	38.98	crystal β		229.25	52.16	313.66	76.87	9.455	1.749	11.849	2.872	107.77	30.07
145.85	39.38	78.30	24.42	231.27	52.55	315.61	77.06	9.869	1.922	12.291	3.072	109.74	30.43
147.83	39.80	80.32	24.81	233.28	52.92	317.56	77.17	10.39	2.151	12.931	3.358	111.70	30.80
149.81	40.20	82.21	25.18	235.29	53.29	319.50	77.33	11.02	2.429	13.573	3.642	113.67	31.16
151.79	40.61	84.10	25.56	237.29	53.61	321.45	77.46	11.65	2.717	14.222	3.944	115.64	31.52
153.76	41.02	86.01	25.93	239.31	53.91	323.39	77.64	12.29	3.012	14.875	4.266	117.61	31.87
155.74	41.44	87.92	26.32	241.31	54.24	325.33	77.76	12.93	3.308	15.641	4.629	119.58	32.24
157.72	41.84	89.85	26.70	243.31	54.55	327.28	77.93	13.57	3.607	16.523	5.061	121.56	32.59
159.70	42.27	91.79	27.08	245.30	54.86	329.22	78.10	14.23	3.914	17.411	5.473	123.54	32.91
161.67	42.72	93.73	27.46	247.29	55.16	331.17	78.24	14.89	4.225	18.299	5.877	125.52	33.27
163.63	43.13	95.69	27.85	249.28	55.44	333.11	78.36	15.66	4.605	19.187	6.282	127.50	33.63
165.60	43.57	97.65	28.22	251.27	55.76	335.06	78.53	16.54	5.037	20.076	6.687	129.48	33.98
167.57	44.02	99.62	28.61	253.26	56.09	337.01	78.69	17.43	5.444	21.275	7.232	131.47	34.32
169.53	44.48	101.60	28.98	255.24	56.44	338.96	78.86	18.31	5.849	22.772	7.903	133.46	34.68
171.49	44.97	103.58	29.34	257.22	56.79	340.91	79.01	19.20	6.248	24.271	8.570	135.45	35.02
173.45	45.49	105.57	29.70	259.20	57.18	342.86	79.16	20.09	6.652	25.766	9.208	137.44	35.37
175.41	46.05	107.56	30.08	261.17	57.65	344.81	79.30	21.29	7.181	27.269	9.818	139.43	35.73
177.36	46.77	109.57	30.44	263.13	58.09	346.77	79.47	22.79	7.851	28.785	10.42	141.43	36.07
179.30	47.60	111.58	30.80	265.09	58.69	348.73	79.62	24.29	8.509	30.296	11.03	143.43	36.43
181.23	48.91	113.59	31.16	268.15	83.95	350.69	79.80	25.79	9.143	31.803	11.62	145.42	36.78
183.12	51.49	115.60	31.51	liquid		352.64	79.96	27.29	9.753	33.307	12.17	147.42	37.13
184.88	59.88	117.62	31.86	274.24	73.87	354.60	80.11	28.81	10.37	34.809	12.69	149.42	37.48
186.45	68.84	119.64	32.21	277.08	74.11	356.56	80.28	30.32	10.96	36.313	13.21	151.42	37.84
liquid		121.66	32.58	279.01	74.28	358.51	80.44	31.83	11.54	37.820	13.71	153.42	38.19
188.06	68.80	123.69	32.94	280.94	74.40	360.47	80.60	33.34	12.09	39.332	14.21	155.42	38.55
189.67	68.87	125.72	33.28	282.88	74.53	362.43	80.77	34.84	12.63	41.115	14.78	157.43	38.91
191.28	68.93	127.75	33.64	284.82	74.67	364.38	80.91	36.34	13.14	43.177	15.43	159.43	39.26
192.89	69.01	129.78	33.99	286.75	74.79	366.34	81.08	37.85	13.65	45.256	16.07	161.44	39.62
194.51	69.11	131.82	34.34	288.69	74.96	368.29	81.23	39.36	14.16	47.350	16.70	163.44	39.98
196.13	69.18	133.85	34.69	290.62	75.09	series 6		40.88	14.64	49.427	17.31	165.45	40.35
197.75	69.26	135.89	35.04	292.56	75.24	supercooled liquid		42.41	15.11	51.466	17.91	167.46	40.71
199.37	69.33	137.93	35.39	294.50	75.39	239.34	71.50	43.95	15.61	53.458	18.48	169.47	41.07
201.12	69.43	139.97	35.73	296.43	75.57	241.35	71.64	45.51	16.09	55.405	19.05	171.48	41.44
203.00	69.55	142.02	36.09	298.37	75.72	243.26	71.77	47.06	16.56	57.318	19.59	173.49	41.82
crystal β		144.06	36.44	286.75	74.79	245.18	71.89	48.60	17.03	59.224	20.08	175.51	42.20
254.94	56.25	146.11	36.80	288.69	74.96	247.09	72.04	50.13	17.45	61.152	20.56	177.52	42.57
257.07	56.67	148.15	37.15	290.62	75.09	249.01	72.15	51.62	17.89	63.133	21.05	179.53	42.95
259.18	57.10	150.19	37.52	292.56	75.24	250.93	72.27	53.10	18.29	65.192	21.57	181.55	43.34

Table 2. (Continued)

⟨*T*⟩	$C_{s,m}$[a]	⟨*T*⟩	$C_{s,m}$[a]	⟨*T*⟩	$C_{s,m}$[a]	⟨*T*⟩	$C_{s,m}$[a]	⟨*T*⟩	$C_{s,m}$[a]	⟨*T*⟩	$C_{s,m}$[a]	⟨*T*⟩	$C_{s,m}$[a]
K	*R*	K	*R*	K	*R*	K	*R*	K	*R*	K	*R*	K	*R*
183.56	43.73	141.39	36.00	liquid		158.84	39.02	262.85	58.33	242.55	53.88	253.35	56.85
185.58	44.10	143.17	36.30	272.04	73.71	160.74	39.36	264.91	59.18	244.36	54.14	255.24	57.19
187.59	44.50	144.95	36.61	275.33	73.99	162.64	39.69	266.94	62.12	246.18	54.45	257.14	57.50
189.61	44.90	146.73	36.92	278.62	74.23	164.54	40.02	liquid		247.99	54.76	259.03	57.79
191.62	45.31	148.52	37.23	281.91	74.46	166.44	40.36	273.34	73.79	249.80	55.10	260.92	58.08
193.64	45.73	150.30	37.55	285.19	74.72	168.35	40.69	275.22	73.91	251.60	55.43	262.80	58.46
195.66	46.14	152.09	37.84	288.50	74.94	170.25	41.04	277.14	74.08	253.40	55.79	series 24	
197.67	46.56	153.87	38.15	291.79	75.21	172.16	41.37	279.06	74.21	255.21	56.19	crystal α	
199.69	46.98	155.66	38.48	295.09	75.46	174.06	41.72	series 18		257.15	56.71	131.44	34.25
201.70	47.46	157.44	38.79	298.38	75.69	175.97	42.06	supercooled liquid		259.28	57.31	133.43	34.60
203.72	47.92	159.23	39.09	301.68	75.93	177.88	42.40	200.44	69.40	261.37	58.00	135.42	34.94
205.73	48.39	161.03	39.42	304.97	76.17	179.78	42.74	202.21	69.53	263.44	58.85	137.41	35.27
207.75	48.80	162.82	39.74	308.26	76.43	181.69	43.11	203.91	69.59	265.47	60.02	139.41	35.63
209.77	49.36	164.61	40.05	311.55	76.70	183.60	43.45	205.60	69.68	series 21		141.40	35.97
211.79	49.91	166.40	40.34	314.84	76.94	185.51	43.80	207.30	69.78	supercooled liquid		143.40	36.33
213.81	50.46	168.19	40.65	318.13	77.20	187.41	44.14	208.99	70.04	204.96	69.62	145.40	36.66
215.83	51.03	169.98	41.00	321.41	77.44	189.32	44.51	series 19		206.75	69.71	147.40	37.00
217.85	51.83	171.78	41.33	324.69	77.68	191.23	44.85	crystal γ		208.56	69.82	149.39	37.36
219.87	52.42	173.57	41.67	327.98	77.97	193.14	45.21	195.46	45.65	210.38	69.94	151.40	37.71
221.89	53.29	175.37	41.98	331.27	78.25	195.05	45.56	197.39	46.00	212.20	70.02	153.41	38.06
223.91	54.29	177.16	42.30	334.56	78.50	196.97	45.92	199.23	46.34	214.02	70.14	155.41	38.42
225.93	55.36	178.96	42.62	337.85	78.79	198.88	46.28	201.07	46.70	series 22		157.42	38.77
227.95	56.31	180.76	42.95	341.19	79.06	200.79	46.65	202.91	47.04	crystal γ		159.43	39.11
229.97	56.72	182.55	43.28	344.49	79.33	202.70	47.04	204.75	47.40	210.42	48.49	161.45	39.46
232.01	56.32	184.35	43.61	347.81	79.62	204.62	47.40	206.59	47.74	212.25	48.80	163.47	39.82
234.05	55.62	186.15	43.94	351.12	79.90	206.54	47.78	208.43	48.09	214.08	49.15	165.48	40.16
236.09	55.16	187.94	44.26	354.43	80.15	208.45	48.14	210.27	48.43	215.91	49.48	167.49	40.53
238.13	55.19	189.74	44.59	357.74	80.45	210.37	48.49	212.10	48.79	217.74	49.86	169.50	40.89
240.17	55.06	191.53	44.92	361.05	80.72	212.29	48.86	213.93	49.15	219.57	50.18	171.51	41.24
242.21	55.20	193.33	45.31	364.36	80.99	214.21	49.22	215.77	49.48	221.39	50.49	173.53	41.61
244.27	55.62	195.13	45.57	367.68	81.28	216.13	49.59	217.60	49.81	223.21	50.83	175.55	41.96
246.37	55.41	196.93	45.96	series 16		218.06	49.96	219.43	50.13	225.04	51.16	177.57	42.34
248.53	51.92	198.73	46.29	crystal β		219.98	50.31	221.25	50.47	226.86	51.47	179.59	42.70
250.66	52.94	200.52	46.61	78.55	24.45	221.90	50.65	223.08	50.79	228.69	51.77	181.61	43.07
252.68	55.82	202.31	46.98	80.51	24.83	223.83	51.03	224.91	51.09	230.50	52.05	183.62	43.46
254.69	56.18	204.11	47.32	82.33	25.20	225.75	51.43	226.73	51.43	232.31	52.35	185.65	43.81
256.72	56.67	205.91	47.61	84.15	25.57	227.68	51.76	228.55	51.75	234.13	52.60	187.67	44.19
258.74	57.11	207.71	47.99	85.98	25.93	229.61	52.15	230.37	52.02	235.95	52.84	189.69	44.57
series 14		209.51	48.36	87.80	26.29	231.54	52.50	232.19	52.30	237.76	53.07	191.71	44.94
crystal γ		211.31	48.68	89.63	26.66	233.46	52.87	234.01	52.58	239.58	53.35	193.74	45.31
78.29	24.41	213.12	49.00	91.46	27.02	235.39	53.20	235.83	52.82	241.40	53.62	195.77	45.70
80.14	24.78	214.92	49.32	93.30	27.38	237.32	53.51	237.65	53.08	243.21	53.89	197.79	46.09
81.86	25.11	216.73	49.66	95.14	27.74	239.25	53.85	239.46	53.35	245.02	54.15	199.81	46.48
83.57	25.46	218.53	50.01	96.97	28.10	241.18	54.16	241.28	53.61	246.84	54.50	201.84	46.89
85.29	25.80	220.34	50.31	98.82	28.47	243.11	54.44	243.10	53.88	248.64	54.82	203.87	47.25
87.00	26.12	222.15	50.65	100.66	28.82	245.05	54.80	244.91	54.16	250.45	55.16	205.90	47.64
88.72	26.47	223.95	50.96	102.51	29.14	246.98	55.06	246.73	54.48	252.25	55.52	207.93	48.03
90.45	26.83	225.76	51.28	104.36	29.49	248.91	55.32	248.54	54.82	254.05	55.94	209.95	48.42
92.18	27.16	227.57	51.59	106.21	29.83	250.85	55.62	250.35	55.17	255.85	56.39	211.98	48.81
93.91	27.51	229.38	51.92	108.07	30.16	252.78	55.97	252.15	55.52	257.82	56.96	214.01	49.19
95.64	27.85	231.19	52.19	109.93	30.50	254.71	56.31	253.96	55.96	259.92	57.67	216.05	49.57
97.38	28.18	233.00	52.46	111.79	30.84	series 17		series 20		262.01	58.31	218.08	49.98
99.12	28.52	234.81	52.75	113.65	31.17	crystal β		crystal γ		264.07	59.17	220.12	50.34
100.86	28.83	236.62	53.03	115.52	31.50	218.19	49.97	200.44	46.57	series 23		222.16	50.76
102.60	29.16	239.39	53.44	117.38	31.82	220.22	50.36	202.38	46.92	crystal α		224.20	51.17
104.34	29.48	241.28	53.76	119.25	32.15	222.16	50.72	204.22	47.30	212.91	49.00	226.24	51.56
106.09	29.81	243.10	54.03	121.12	32.48	224.09	51.08	206.06	47.66	214.94	49.37	228.28	52.01
107.84	30.14	244.91	54.34	122.99	32.81	226.01	51.46	207.90	48.00	216.88	49.74	230.32	52.41
109.59	30.44	246.72	54.64	124.86	33.12	227.94	51.84	209.73	48.31	218.82	50.12	232.36	52.84
111.34	30.76	248.53	54.95	126.74	33.46	229.86	52.25	211.57	48.64	220.76	50.48	234.40	53.25
113.09	31.08	250.35	55.28	128.61	33.79	231.79	52.58	213.40	49.01	222.70	50.88	236.44	53.64
114.85	31.38	252.16	55.63	130.49	34.12	233.71	52.96	215.24	49.37	224.63	51.26	238.48	54.08
116.61	31.69	253.97	56.04	132.37	34.43	235.63	53.31	217.07	49.74	226.56	51.63	240.53	54.48
118.37	31.99	liquid		134.25	34.75	237.54	53.61	218.90	50.04	228.49	52.02	242.57	54.84
120.13	32.30	274.89	73.97	136.14	35.07	239.46	53.92	220.72	50.40	230.41	52.42	244.61	55.22
121.89	32.62	276.80	74.09	138.03	35.40	241.38	54.20	222.55	50.74	232.33	52.81	246.66	55.59
123.65	32.93	278.72	74.27	139.91	35.73	243.29	54.47	224.37	51.08	234.25	53.19	248.70	55.99
125.42	33.24	280.64	74.39	141.80	36.05	245.20	54.76	226.20	51.40	236.17	53.56	250.75	56.37
127.19	33.54	282.55	74.52	143.69	36.38	247.11	55.09	228.02	51.69	238.09	53.96	252.79	56.73
128.96	33.84	284.47	74.68	145.58	36.70	249.03	55.34	229.84	51.97	240.00	54.33	254.83	57.09
130.73	34.16	286.38	74.76	147.47	37.03	250.94	55.67	231.66	52.28	241.92	54.69	256.88	57.43
132.51	34.47	288.30	74.97	149.36	37.36	252.85	55.96	233.48	52.57	243.83	55.05	258.93	57.78
134.29	34.76	series 15		151.26	37.69	254.75	56.27	235.29	52.85	245.74	55.43	260.97	58.20
136.07	35.08	supercooled liquid		153.15	38.02	256.65	56.63	237.11	53.12	247.64	55.80	260.97	58.20
137.84	35.37	266.18	73.30	155.05	38.35	258.65	57.05	238.92	53.38	249.55	56.17	263.01	58.82
139.62	35.67	268.75	73.50	156.94	38.69	260.76	57.64	240.74	53.61	251.45	56.53	265.04	59.82

Table 2. (Continued)

⟨T⟩ / K	$C_{s,m}$[a] / R	⟨T⟩ / K	$C_{s,m}$[a] / R	⟨T⟩ / K	$C_{s,m}$[a] / R	⟨T⟩ / K	$C_{s,m}$[a] / R	⟨T⟩ / K	$C_{s,m}$[a] / R	⟨T⟩ / K	$C_{s,m}$[a] / R	⟨T⟩ / K	$C_{s,m}$[a] / R
267.06	63.56	97.94	28.29	127.07	33.51	156.87	38.68	186.64	44.00	216.04	49.63	245.09	55.30
268.84	116.2	99.75	28.63	129.05	33.85	158.86	39.02	188.61	44.37	217.99	49.99	247.01	55.62
series 25		101.63	28.97	131.03	34.20	160.85	39.37	190.58	44.73	219.93	50.37	248.93	56.01
crystal α		103.56	29.33	133.01	34.54	162.84	39.72	192.55	45.11	221.88	50.75	250.85	56.35
78.32	24.41	105.50	29.70	135.00	34.89	164.83	40.06	194.52	45.49	223.82	51.12	252.77	56.69
80.18	24.76	107.44	30.04	136.98	35.23	166.82	40.42	196.48	45.87	225.76	51.51	254.69	57.02
81.93	25.12	109.39	30.41	138.97	35.56	168.80	40.77	198.45	46.25	227.70	51.92	256.87	57.49
83.68	25.46	111.34	30.75	140.96	35.91	170.80	41.12	200.41	46.60	229.64	52.29	259.39	57.98
85.43	25.80	113.29	31.10	142.95	36.25	172.78	41.48	202.37	47.01	231.57	52.69	261.89	58.65
87.20	26.16	115.25	31.46	144.94	36.59	174.77	41.84	204.32	47.38	233.52	53.09	264.38	59.79
88.97	26.52	117.22	31.80	146.92	36.94	176.75	42.19	206.28	47.76	235.45	53.47	266.87	64.10
90.75	26.87	119.18	32.14	148.91	37.29	178.73	42.55	208.23	48.13	237.38	53.87	268.93	131.2
92.54	27.23	121.15	32.49	150.91	37.64	180.71	42.91	210.19	48.50	239.31	54.25		
94.33	27.58	123.12	32.83	152.90	37.99	182.69	43.26	212.14	48.88	241.24	54.62		
96.14	27.93	125.10	33.18	154.88	38.32	184.66	43.63	214.09	49.26	243.16	54.95		

[a] Average heat capacity at the mean temperature of an experiment.

ments, sample 1 of 1.1769 g mass in series 1 to 11, and sample 2 of 0.6579 g mass in series 12 to 25. The history of calorimetric measurements, procedures for preparation of phases, and temperature ranges of the measurements are shown in Table 3.

Glass, Supercooled Liquid. Liquid [C_6mim][NTf_2] at cooling from 300 K with initial rate of (0.02 to 0.03) K·s^{-1} can be easily supercooled and forms a glass phase. Heat capacities of the glass were measured in series 1, 2, and 11 (Tables 2 and 3). Devitrification of the sample occurred in the temperature range of (173 to 188) K (Figure 8).

Heat capacity of the supercooled liquid (above T_g) was measured from the temperatures just above the transition "glass → supercooled liquid" to the temperatures at which a spontaneous crystallization occurred: 204 K for sample 1 (series 2) and (209 to 210) K for sample 2 (series 12 and 18). At higher temperatures, the heat capacity of the supercooled liquid was measured in the experiment carried out just after cooling of the liquid below T_{fus} (series 5 to 9, 15, and 21). On supercooling the liquid to 231 K, the formed metastable phase is stable enough to perform calorimetric measurements (series 5 to 7 with repeating cooling−measuring cycles). On cooling the liquid below 225 K (but above the glass transirion range), crystallization of the supercooled phase occurs only after a time long enough to carry out two to six calorimetric experiments for heat capacity measurements (series 8, 9, and 21). Such a feature in the thermal behavior of supercooled [C_6mim][NTf_2] allowed us to measure its heat capacity almost all over the range (T_g to T_{fus}) (excluding the small temperature range of (226 to 233) K).

The temperature corresponding to the average heat capacity of the substance in the glass transition range was assumed to be the glass transition temperature:

$$T_g = (184.3 \pm 0.1)\ \mathrm{K}$$

The heat capacity jump at the transition "glass → supercooled liquid" was determined as the heat capacity difference between the supercooled liquid and the glass at T_g:

$$\Delta^{l}_{gl}C_{s,m} \cong \Delta^{l}_{gl}C_{p,m} = C_{s,m}(\mathrm{sup.liq};\ T_g) - C_{s,m}(\mathrm{gl};\ T_g) = (170.7 \pm 2.8)\ \mathrm{J{\cdot}K^{-1}{\cdot}mol^{-1}}$$

$C_{s,m}$(gl; T_g) and $C_{s,m}$(sup.liq; T_g) values were calculated from the following equations:

$$C_{s,m}(\mathrm{gl}) = \{243.8 - 0.4568{\cdot}(T/\mathrm{K}) + 7.081{\cdot}10^{-3}{\cdot}(T/\mathrm{K})^2\}\ \mathrm{J{\cdot}K^{-1}{\cdot}mol^{-1}} \quad (1)$$

$$C_{s,m}(\mathrm{sup.liq;\ liq}) = \{547.7 - 0.1153{\cdot}(T/\mathrm{K}) + 1.305{\cdot}10^{-3}{\cdot}(T/\mathrm{K})^2\}\ \mathrm{J{\cdot}K^{-1}{\cdot}mol^{-1}}, \quad (2)$$

obtained from the experimental heat capacities of the glass in a range of temperatures of (150 to 171) K and the liquid in a range of temperatures of (188 to 300) K, respectively.

The residual entropy and the residual enthalpy of the glassy [C_6mim][NTf_2]:

$$S^{o}_{m}(\mathrm{gl},\ T \to 0) = (24.1 \pm 4.1)\ \mathrm{J{\cdot}K^{-1}{\cdot}mol^{-1}}$$

$$H^{o}_{m}(\mathrm{gl},\ T \to 0) = (12.21 \pm 0.59)\ \mathrm{kJ{\cdot}mol^{-1}}$$

were found according to the following equations:

$$S^{o}_{m}(\mathrm{gl},\ T \to 0) = \frac{\Delta_{fus}H^{o}_{m}}{T_{fus}} - \int_{T=0}^{T_{fus}} \frac{C_{p,m}(\mathrm{gl,liq}) - C_{p,m}(\mathrm{cr})}{T'}\,\mathrm{d}T' \quad (3)$$

$$H^{o}_{m}(\mathrm{gl},\ T \to 0) = \Delta_{fus}H^{o}_{m} - \int_{T=0}^{T_{fus}} [C_{p,m}(\mathrm{gl,liq}) - C_{p,m}(\mathrm{cr})]\,\mathrm{d}T' \quad (4)$$

where $C_{p,m}$(cr) and $\Delta_{fus}H^{o}_{m}$ are heat capacity and enthalpy of fusion for the α crystal (see below).

Crystal Phases. Three crystal modifications of [C_6mim][NTf_2] designated as α, *β*, and *γ* (Table 3) were obtained under different thermal conditions of crystallization. In this sequence, the heat capacities of the crystals above 240 K decrease (Figure 9).

β Crystal. Initially, in the experiments with sample 1, the *β* crystal was obtained (series 2 to 4). After spontaneous crystallization had occurred at temperatures above 204 K (series 2), the calorimetric experiments were continued. The temperature step was ≈ 2 K if the phase in the calorimeter was stable. The heat evolution due to crystallization manifested in high-temperature trends was finished at 254 K. In the consequent experiments (series 2), heat capacities of the crystal were measured, and the crystal was melted.

Based on the results from series 2, the following procedure was applied to obtain the crystal [C_6mim][NTf_2]. After the crystallization had begun, the calorimeter with the sample was slowly heated (average rate of 5 mK·s^{-1}) to T = 255 K. This process is designated as "crystallization of supercooled liquid in a range of temperatures of (205 to 255) K" (series 3). The obtained crystal was kept at T = (255 to 256) K for 20 h. The temperature dependence of heat capacity for the *β* crystal at temperatures above 200 K (series 3) was reproduced in a second

Table 3. Description of the Series of Calorimetric Experiments for [C_6mim][NTf_2] in the Condensed State with Indication of the Phases and Temperature Ranges of Heat Capacity Measurements

	preparation procedure			heat capacity measurements	
series	1. formation	2. annealing, heating	3. cooling	phases	temp range
			Sample 1 (m_s = 1.1769 g)		
1	cooling of liquid		from 300 K to 77 K	glass	(79 to 131) K
2	cooling of glass (after series 1)		from 132 K to 125 K at a rate of 0.01 K·s^{-1}	glass	126 K to T_g
				supercooled liquid	T_g to 203 K
				crystal	255 K to T_{fus}
				liquid	T_{fus} to 277 K
3	crystallization of supercooled liquid in temperature range of (205 to 255) K	20 h at (255 to 256) K	to 201 K at a rate of (0.02 to 0.01) K·s^{-1}	crystal β	(202 to 258) K
4	cooling of crystal β (after series 3)		from 259 K to 77 K	crystal β	78 K to T_{fus}
				liquid	T_{fus} to 298 K
5	cooling of liquid		from 300 K to 250 K at a rate of (0.03 to 0.02) K·s^{-1}	supercooled liquid	251 K to T_{fus}
				liquid	T_{fus} to 368 K
6	cooling of liquid		from 370 K to 238 K at a rate of (0.04 to 0.02) K·s^{-1}	supercooled liquid	239 to 259 K
7	cooling of supercooled liquid (after series 6)		from 260 K to 231 K at a rate of 0.02 K·s^{-1}	supercooled liquid	233 to 242 K
8	cooling of supercooled liquid (after series 7)		from 243 K to 223 K at a rate of 0.02 K·s^{-1}	supercooled liquid	224 to 226 K
9	cooling of liquid		from 290 K to 214 K at a rate of (0.03 to 0.02) K·s^{-1}	supercooled liquid	215 to 220 K
10	(like in series 3) crystallization of supercooled liquid in temperature range of (205 to 255) K	20 h at (255 to 256) K	to 77 K (nitrogen bath) and then to 4.8 K (helium bath)	crystal β	5 to 84 K
11	(like in series 1) cooling of liquid		from 300 K to 77 K (nitrogen bath) and then to 4.8 K (helium bath)	glass	5 to 84 K
			Sample 2 (m_s = 0.6579 g)		
12	heating of glass from 78 K to 193 K			supercooled liquid	194 to 208 K
13	crystallization of supercooled liquid in temperature range of (209 to 235) K	20 h at (235 to 236) K	to 77 K	crystal γ, partly amorphous	78 to 259 K
14	cooling of crystal γ (after series 13)		from 260 K to 77 K	crystal γ	78 K to T_{fus}
				liquid	T_{fus} to 288 K
15	cooling of liquid (after series 14)		from 290 K to 265 K at a rate of (0.03 to 0.02) K·s^{-1}	supercooled liquid	266 K − T_{fus}
				liquid	T_{fus} to 368 K
16	crystallization of supercooled liquid in temperature range of (210 to 255) K	45 h at (255 to 257) K	to 77 K	crystal β	78 to 255 K
17	crystal β (after series 16)	18 h at (255 to 256) K	to 217 K at a rate of 0.02 K·s^{-1}	crystal β	218 K to T_{fus}
				liquid	T_{fus} to 279 K
18	heating of glass from 100 K to 199 K			supercooled liquid	200 to 209 K
19	crystallization of supercooled liquid in temperature range of (210 to 235) K	18 h at (235 to 236) K, then heating to 254 K at a rate of 0.005 K·s^{-1}	to 194 K at a rate of 0.02 K·s^{-1}	crystal γ	195 to 254 K
20	crystal γ (after series 19)	10 h at 255 K	to 199 K at a rate of 0.02 K·s^{-1}	crystal γ	200 to T_{fus}
21	cooling of liquid (after series 20)		from 275 K to 204 K at a rate of (0.03 to 0.02) K·s^{-1}	supercooled liquid	205 to 214 K
22	crystallization of supercooled liquid in temperature range of (214 to 236) K	68 h at (236 to 238) K, then heating to 256 K at a rate of 0.005 K·s^{-1}	to 209 K at a rate of 0.02 K·s^{-1}	crystal γ	210 to 264 K
23	crystal γ (after series 22)	5 h at 265 K	to 250 K at a rate of 0.002 K·s^{-1}, then to 212 K at a rate of 0.02 K·s^{-1}	crystal α	213 to 263 K
24	crystallization of supercooled liquid in temperature range of (210 to 269) K	10 h at 269 K	to 250 K at a rate of 0.001 K·s^{-1}, then to 130 K at a rate of 0.02 K·s^{-1}	crystal α	131 to T_{fus}
25	crystallization of supercooled liquid in temperature range of (210 to 269) K	18 h at 269 K	to 250 K at a rate of 0.001 K·s^{-1}, then to 77 K	crystal α	78 to T_{fus}

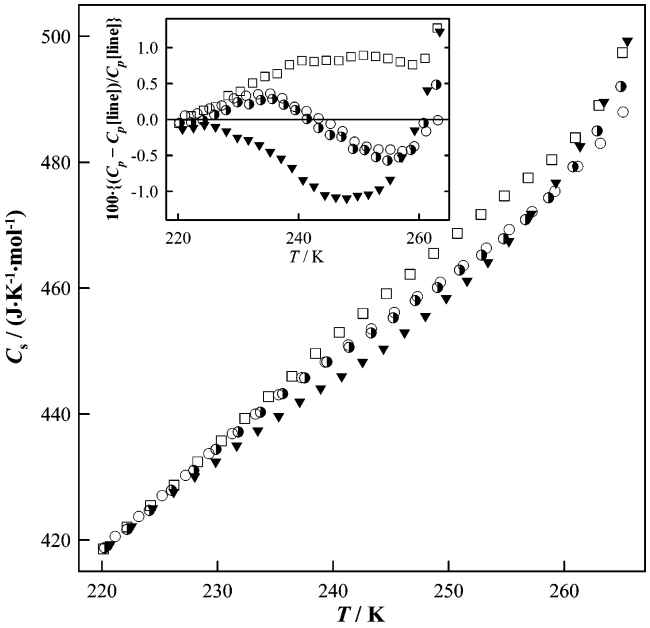

Figure 9. Heat capacities of different crystal phases of $[C_6mim][NTf_2]$ above 220 K: □, crystal α (series 24, sample 2); ○, crystal β (series 4, sample 1); ◑, crystal β (series 17, sample 2); ▼, crystal γ (series 20, sample 2). Inset: Percentage deviations of the heat capacities (C_p) of different crystal phases from the values C_p[line] obtained by equation $C_p/(J{\cdot}K^{-1}{\cdot}mol^{-1}) = 86.35 + 1.508{\cdot}(T/K)$.

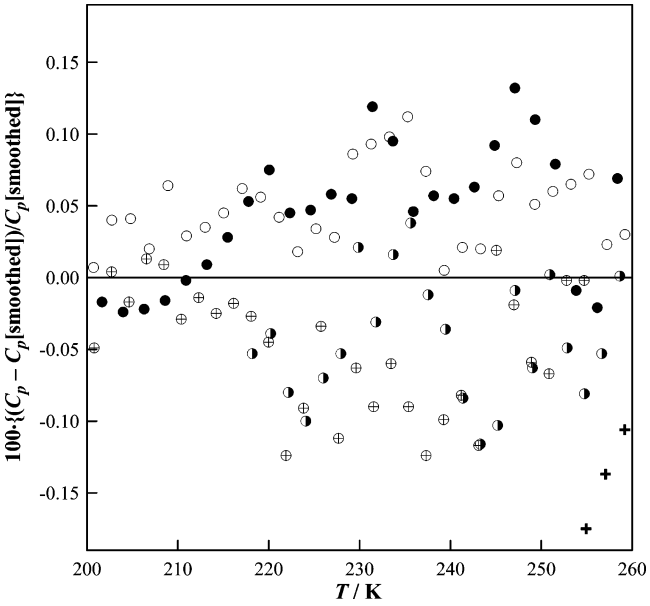

Figure 10. Percentage deviations of the heat capacities of the β crystal from the smoothed polinomial functions in the temperature range of (200 to 260) K: +, series 2 (sample 1); ●, series 3 (sample 1); ○, series 4 (sample 1); ⊕, series 16 (sample 2); ◑, series 17 (sample 2).

pass through this region after heating the crystal to 260 K (series 4). The experimental heat capacities from series 3 and 4 agree to within 0.1 %.

A similar procedure was applied to obtain the β crystal for sample 2 (series 16). An additional keeping of the β crystal at the temperatures of (255 to 256) K for 18 h had no significant effect on the heat capacity of the crystal (Figure 10). Heat capacities from series 16 and 17 agree to within 0.15 %. Deviations of the heat capacities of the β crystal for different samples does not exceed 0.25 % above 200 K and 0.1 % at T = (80 to 200) K. These are comparable with reproducibility of the results with this calorimeter.

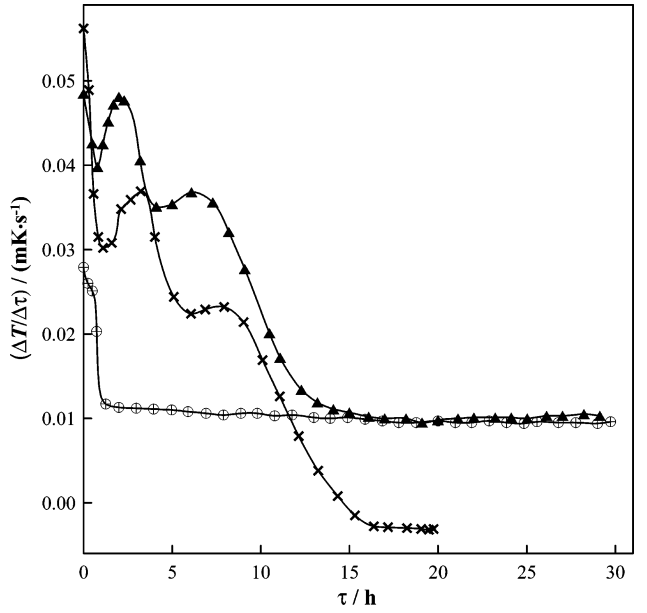

Figure 11. Time dependence of temperature drifts of the calorimeter during formation of the crystal phases of $[C_6mim][NTf_2]$: ×, γ crystal, partly amorphous (series 13, annealing at (235 to 236) K); ⊕, β crystal (series 16, annealing at (255 to 257) K); ▲, γ crystal (series 22, annealing at (236 to 238) K).

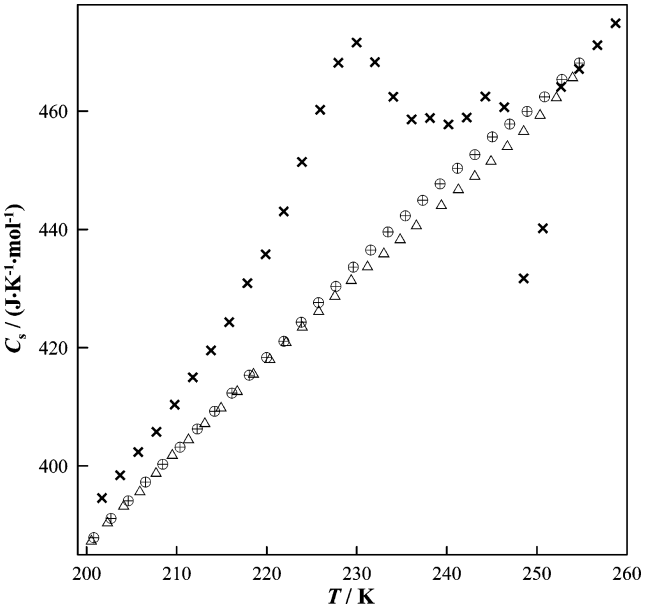

Figure 12. Heat capacities of selected crystalline phases of $[C_6mim][NTf_2]$ at T > 200 K (sample 2): ×, crystal γ, partly amorphous (series 13); △, crystal γ (series 14); ⊕, crystal β (series 16).

γ Crystal. Above 200 K an anomaly with a weak maximum near (230 to 240) K occurs in the temperature dependence of the heat capacity for the β crystal (Figures 8 and 9). The second pass in the range (series 3 and 4, Figure 10) does not affect this anomaly and heat capacities of the β crystal. To explore the nature of this anomaly, the crystallization process was carried out in such a way that the maximum temperature did not exceed (235 to 236) K. To prevent overheating caused by the crystallization, sample 2 with the lower mass was used in series 12 to 25 (Tables 2 and 3).

In series 13 when the crystallization process started at temperatures above 209 K, the calorimeter with the sample was slowly (average rate 5 mK·s^{-1}) heated to $T \approx 220$ K at which point the quick crystallization started. The following increase

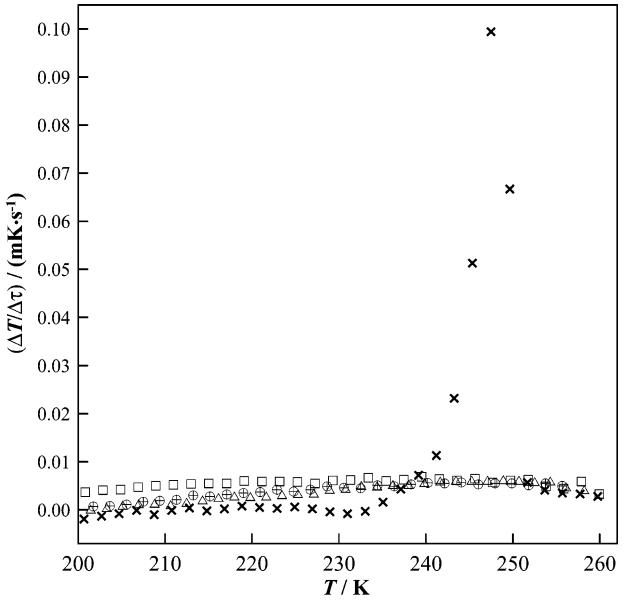

Figure 13. Temperature drifts during the heat capacity measurements of crystal phases for $[C_6mim][NTf_2]$ in the temperature range of (200 to 260) K (sample 2): ×, γ crystal, partly amorphous (series 13); △, γ crystal (series 14); ⊕, β crystal (series 16); □, α crystal (series 24).

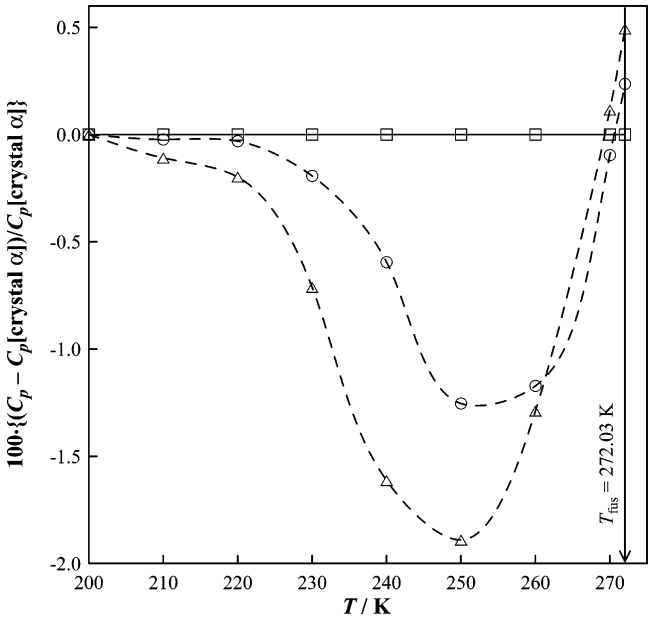

Figure 14. Percentage deviations of the smoothed and extrapolated (above 260 K) values of the heat capacities of the β crystal and the γ crystal from those for the α crystal: □, α crystal; ○, β crystal; △, γ crystal.

of the temperature of the calorimeter with the sample to (235 to 236) K was caused by the energy evolved during the crystallization process. This procedure is called "crystallization of supercooled liquid in a range of temperatures of (209 to 235) K". The sample was then annealed at T = (235 to 236) K for 20 h until the temperature trend of the calorimeter became constant (Figure 11). Then it was cooled to 77 K. A peak with a maximum at 230 K (Figure 12) was observed in the temperature dependence of the heat capacity of the obtained crystal designated as the γ crystal, partly amorphous. The measurements in the temperature range of (230 to 250) K were accompanied by additional heat release due to completion of crystallization of the sample. This was monitored by high positive temperature trends of the calorimeter (Figure 13). At temperatures above 250 K the temperature trends became normal

Table 4. Determination of the Molar Enthalpy of Fusion for $[C_6mim][NTf_2]$

series number or way of formation, sample number[a]	T_{start} / K	T_{end} / K	Q / J·mol^{-1}	$\Delta_{fus}H^o_m$ / J·mol^{-1}
	Crystal α			
series 24, no. 2	256.21	273.42	36635	28062[b]
series 25, no. 2	256.25	272.49	36106	28123[c]
like in series 25, no. 2	255.81	275.68	38245	28089[c]
				(28091 ± 76)[d]
	Crystal β			
series 4, no. 1	258.36	273.64	35784	28149[b]
like in series 3, no. 1	258.87	275.94	36967	28159 [b]
like in series 3, no. 1	259.70	273.85	35338	28210[c]
like in series 3, no. 1	258.46	272.78	35197	28137 [c]
series 17, no. 2	255.85	272.91	36554	28182[b]
				(28167 ± 36)[d]
	Crystal γ			
series 14, no. 2	255.79	274.18	37436	28255 [c]
series 20, no. 2	254.49	273.39	37598	28294[b]
like in series 19, no. 2	253.35	274.04	38508	28275[c]
				(28275 ± 48)[d]

[a] Sample number: no. 1 for the sample with m_s = 1.1769 g; no. 2 for the sample with m_s = 0.6579 g. [b] From the fractional melting experiments. [c] From independent single-step experiments. [d] Average value.

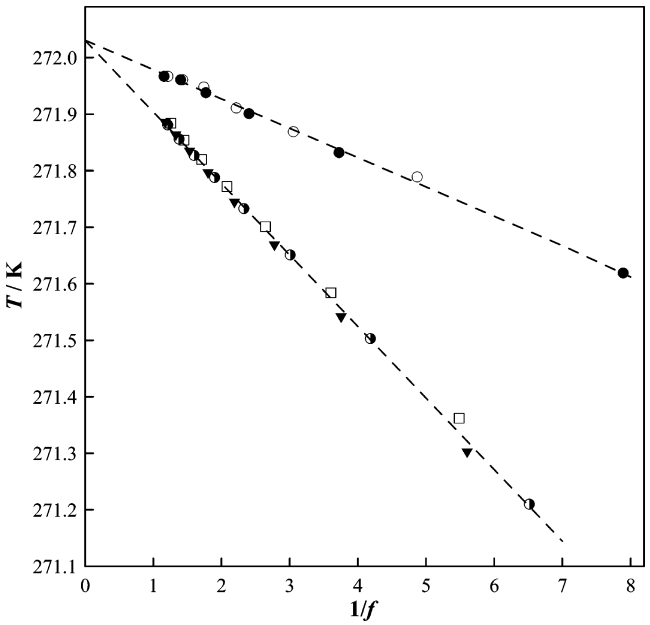

Figure 15. Results of the fractional-melting experiments for $[C_6mim][NTf_2]$: ○, series 1 for the β crystal (sample 1); ●, series 2 for the β crystal (sample 1); □, α crystal (sample 2); ◑, β crystal (sample 2); ▼, γ crystal (sample 2).

(Figure 13), and the heat capacities of the crystal phase became close to those for the β crystal (Figure 12).

No anomalies except that for fusion were found in the temperature curve of the heat capacity for the γ crystal (Figure 12, series 14). Temperature trends of the calorimeter at T > 200 K are normal (Figure 13). Heat capacities of the substance measured in series 13 and 14 differ significantly (Figure 12).

Taking into account the above-mentioned, the following procedure was applied to get the γ crystal. After annealing at T = (235 to 238) K, the sample was slowly heated (average rate of 5 mK·s^{-1}) to T = (254 to 256) K (series 19 and 22, Table 3). The temperature dependence of the heat capacity for the γ crystal was reproducible after additional annealing for 10 h at T = 255 K (series 19 and 20, Tables 2 and 3). Differences in

Table 5. Enthalpy Increase Caused by the Heating of Crystal from $T = 200$ K to T_{fus} and by the Fusion of Crystal with Formation of Liquid at $T_{fus} = 272.03$ K

value	crystal α	crystal β	crystal γ
$\int_{200}^{T_{fus}} C_{p,m}(\mathrm{cr})\, dT/\mathrm{J\cdot mol^{-1}}$	$\gamma 32011 \pm 35^a$	31851 ± 38^a	31743 ± 53^a
$\Delta_{fus}H_m^o/\mathrm{J\cdot\ mol^{-1}}$	28091 ± 76^a	28167 ± 36^a	28275 ± 48^a
$[H_m^o(\mathrm{liq};\ T_{fus}) - H_m^o(\mathrm{cr};\ 200\ \mathrm{K})]/\mathrm{J\cdot mol^{-1}}$	60102 ± 111^b	60018 ± 74^b	60018 ± 101^{ba}

[a] Random uncertainty. [b] Sum of uncertainties given in the cells above.

Table 6. Results of Fractional-Melting Experiments for [C_6mim][NTf_2][a]

sample 1 with $m_s = 1.1769$ g		sample 2 with $m_s = 0.6579$ g	
T/K	f	T/K	f
crystal β		crystal α	
series 1		271.362	0.1823
271.789	0.2053	271.584	0.2774
271.869	0.3274	271.701	0.3780
271.911	0.4511	271.772	0.4811
271.948	0.5748	271.820	0.5854
271.961	0.6997	271.854	0.6904
271.967	0.8246	271.884	0.7957
$T_0 = (272.03 \pm 0.02)$ K		$T_0 = (272.03 \pm 0.01)$ K	
$x = (0.9977 \pm 0.0003)$		$x = (0.9944 \pm 0.0002)$	
series 2		crystal β	
271.619	0.1267	271.210	0.1535
271.832	0.2685	271.503	0.2390
271.901	0.4161	271.651	0.3325
271.938	0.5648	271.733	0.4295
271.961	0.7145	271.788	0.5265
271.967	0.8646	271.827	0.6259
$T_0 = (272.03 \pm 0.01)$ K		271.856	0.7258
$x = (0.9976 \pm 0.0001)$		271.881	0.8259
		$T_0 = (272.03 \pm 0.01)$ K	
		$x = (0.9942 \pm 0.0001)$	
		crystal γ	
		271.300	0.1785
		271.539	0.2662
		271.666	0.3601
		271.742	0.4568
		271.794	0.5547
		271.832	0.6534
		271.861	0.7525
		271.883	0.8521
		$T_0 = (272.03 \pm 0.01)$ K	
		$x = (0.9940 \pm 0.0001)$	

[a] f is the melting fraction at temperature T; T_0 is the triple point of the compound and x is the mole-fraction purity of the sample

heat capacities of the γ crystal from series 14, 19, 20, and 22 do not exceed 0.4 % in the range of (200 to 255) K where the sample does not start to melt.

α *Crystal.* The β and γ crystals are stable at heating to (255 to 260) K. Additional annealing of the phases at (255 to 256) K (series 17 for the β crystal and series 20 for the γ crystal) does not affect neither the temperature dependence of the heat capacity nor the heat capacities themselves (e.g., Figures 9 and 10 for the β crystal). Moreover, no transition from one crystal to another occurs below 260 K.

However, heating of the γ crystal above 260 K and annealing at $T = 265$ K for 5 h (series 22 and 23) the α crystal which has the highest heat capacities at $T > 200$ K was obtained (Figure 9). The α crystal was also obtained from the supercooled liquid. To do this the calorimeter was slowly (average rate of 5 mK·s^{-1}) heated to 269 K (series 24 and 25, "crystallization of supercooled liquid in a range of temperatures of (210 to 269) K)", and then it was kept at this temperature for 10 h (series 24) and 18 h (series 25). The heat capacities of the α crystal obtained from the γ crystal (series 23) and from the supercooled liquid (series 24 and 25) agree within 0.2 % in the range of temperatures of (200 to 260) K.

Table 7. Molar Thermodynamic Functions of [C_6mim][NTf_2] in the Glassy and Supercooled Liquid States ($R = 8.314472$ J·K^{-1}·mol^{-1})

T	$C_{p,m}$	$\Delta_0^T H_m^o$	$\Delta_0^T S_m^o$	Φ_m^o [b]
K	R	RT	R	R
		Glass		
5	0.3992	0.1024	0.1370	0.03458
10	2.072	0.6300	0.8733	0.2433
15	4.321	1.477	2.129	0.6515
20	6.650	2.484	3.696	1.212
25	8.880	3.543	5.423	1.880
30	10.91	4.604	7.223	2.620
35	12.77	5.640	9.048	3.408
40	14.42	6.636	10.86	4.226
45	15.98	7.588	12.65	5.063
50	17.49	8.503	14.41	5.910
60	20.27	10.24	17.85	7.616
70	22.77	11.85	21.17	9.317
80	25.20	13.37	24.37	11.00
90	27.47	14.81	27.47	12.66
100	29.73	16.19	30.48	14.29
110	31.93	17.52	33.42	15.90
120	34.06	18.81	36.29	17.48
130	36.13	20.06	39.10	19.03
140	38.18	21.29	41.85	20.56
150	40.24	22.48	44.55	22.07
160	42.34	23.65	47.22	23.56
170	44.60	24.82	49.85	25.03
180	48.02	26.00	52.48	26.48
184.3	55.16	26.57	53.67	27.10
		Supercooled Liquid		
190	68.90	27.75	55.68	27.93
200	69.38	29.82	59.22	29.41
210	69.88	31.71	62.62	30.91
220	70.42	33.46	65.88	32.42
230	(70.99)[a]	35.08	69.03	33.95
240	71.59	36.59	72.06	35.47
250	72.22	38.00	74.99	36.99
260	72.88	39.33	77.84	38.51
270	73.57	40.58	80.60	40.02
		Liquid		
272.03	73.72	40.83	81.16	40.32

[a] Interpolated value. [b] Φ_m^o is $\Phi_m^o = -[G_m^o(T) - H_m^o(0)]/T = \Delta_0^T S_m^o - \Delta_0^T H_m^o/T$.

It should be noted that the heat capacities for all the crystal phases of [C_6mim][NTf_2] coincide within 0.1 % in the temperature range (80 to 220) K but they are substantially different at $T > 220$ K (Figures 9 and 14). This difference exceeds experimental error.

Fusion. The enthalpy of fusion was determined for every crystal phase both in special experiments with a continuous heat input and from fractional-melting experiments (Table 4). Initial T_{start} and final T_{end} temperatures of the experiments with continuous heat input lay out of the range of the phase transition. The enthalpy of fusion was calculated from the equation:

Table 8. Molar Thermodynamic Functions of $[C_6mim][NTf_2]$ in the Crystalline and Liquid States ($R = 8.314472$ J·K^{-1}·mol^{-1})

T/K	$C_{p,m}/R$	$\Delta_0^T H_m^o/RT$	$\Delta_0^T S_m^o/R$	Φ_m^o [b]$/R$	T/K	$C_{p,m}/R$	$\Delta_0^T H_m^o/RT$	$\Delta_0^T S_m^o/R$	Φ_m^o [b]$/R$
				Crystal					
5	0.2853	0.06754	0.08929	0.02175	90	26.73	14.63	27.07	12.44
10	1.980	0.5508	0.7388	0.1880	100	28.67	15.94	29.99	14.05
15	4.289	1.406	1.970	0.5647	110	30.52	17.18	32.81	15.62
20	6.614	2.421	3.527	1.106	120	32.29	18.37	35.54	17.17
25	8.805	3.480	5.240	1.760	130	34.02	19.51	38.19	18.69
30	10.84	4.540	7.028	2.488	140	35.74	20.60	40.78	20.17
35	12.68	5.573	8.839	3.266	150	37.47	21.67	43.30	21.63
40	14.36	6.568	10.64	4.075	160	39.22	22.71	45.78	23.06
45	15.93	7.521	12.43	4.904	170	40.99	23.74	48.21	24.47
50	17.42	8.437	14.18	5.745	180	42.79	24.74	50.60	25.86
60	20.15	10.17	17.61	7.438	190	44.63	25.74	52.96	27.22
70	22.49	11.76	20.89	9.127	200	46.52	26.73	55.30	28.57
80	24.72	13.25	24.04	10.80					
				Crystal α					
210	48.44	27.72	57.62	29.89	250	56.23	31.66	66.72	35.06
220	50.36	28.71	59.91	31.21	260	(58.00)[a]	32.64	68.96	36.32
230	52.36	29.69	62.20	32.50	270	(59.68)[a]	33.61	71.19	37.57
240	54.35	30.68	64.47	33.79	272.03	(60.00)[a]	33.81	71.63	37.82
				Liquid					
272.03	73.72	46.23	84.05	37.83	320	77.36	50.62	96.31	45.69
280	74.30	47.02	86.19	39.17	330	78.15	51.44	98.70	47.26
290	75.05	47.97	88.81	40.84	340	78.95	52.24	101.0	48.81
298.15	75.68	48.72	90.90	42.18	350	79.76	53.01	103.3	50.34
300	75.82	48.89	91.37	42.48	360	80.59	53.77	105.6	51.84
310	76.58	49.77	93.87	44.10	370	(81.43)[a]	54.50	107.8	53.32
				Crystal β					
210	48.43	27.72	57.62	29.89	250	55.52	31.63	66.69	35.06
220	50.34	28.71	59.91	31.21	260	(57.32)[a]	32.58	68.90	36.32
230	52.26	29.69	62.19	32.50	270	(59.62)[a]	33.54	71.11	37.57
240	54.02	30.67	64.46	33.79	272.03	(60.14)[a]	33.74	71.56	37.82
				Liquid (from Crystal β)					
272.03	73.72	46.19	84.01	37.82					
				Crystal γ					
210	48.39	27.72	57.61	29.89	250	55.16	31.59	66.64	35.06
220	50.26	28.70	59.91	31.21	260	(57.25)[a]	32.53	68.85	36.31
230	51.99	29.68	62.18	32.50	270	(59.74)[a]	33.49	71.05	37.56
240	53.47	30.64	64.43	33.79	272.03	(60.30)[a]	33.69	71.50	37.81
				Liquid (from Crystal γ)					
272.03	73.72	46.19	84.00	37.81					

[a] Extrapolated values. [b] Φ_m^o is $\Phi_m^o = -[G_m^o(T) - H_m^o(0)]/T = \Delta_0^T S_m^o - \Delta_0^T H_m^o/T$.

$$\Delta_{fus}H_m^o = Q - \int_{T_{start}}^{T_{fus}} C_{p,m}(\text{cr})\,dT - \int_{T_{fus}}^{T_{end}} C_{p,m}(\text{liq})\,dT = Q - q(\text{cr}) - q(\text{liq}) \quad (5)$$

where Q is an energy required to heat 1 mol of substance from T_{start} to T_{end}; q(cr) and q(liq) are energies required to heat 1 mol of the crystal phase from T_{start} to T_{fus} and 1 mol of the liquid phase from T_{fus} to T_{end}, respectively.

Heat capacities of the crystal phases were extrapolated with the equations:

$$C_{p,m}(\text{crystal }\alpha) = \{-181.7 + 3.673\cdot(T/\text{K}) - 4.305\cdot10^{-3}\cdot(T/\text{K})^2\}\ \text{J}\cdot\text{K}^{-1}\cdot\text{mol}^{-1} \quad (6)$$

$$C_{p,m}(\text{crystal }\beta) = \{1421.5 - 8.972\cdot(T/\text{K}) + 20.53\cdot10^{-3}\cdot(T/\text{K})^2\}\ \text{J}\cdot\text{K}^{-1}\cdot\text{mol}^{-1} \quad (7)$$

$$C_{p,m}(\text{crystal }\gamma) = \{1098.9 - 6.696\cdot(T/\text{K}) + 16.54\cdot10^{-3}\cdot(T/\text{K})^2\}\ \text{J}\cdot\text{K}^{-1}\cdot\text{mol}^{-1} \quad (8)$$

obtained by the least-squares fit from experimental heat capacities in the temperature ranges (224 to 259) K (α crystal), (245 to 259) K (β crystal), and (233 to 254) K (γ crystal). The temperature ranges were chosen in such a way to get close (within 0.5 %) heat capacities for all the crystal phases at T_{fus} (Figure 14).

One may see from Table 4 that the enthalpy of fusion increases slightly in a sequence α → β → γ from (28.09 ± 0.08) kJ·mol^{-1} to (28.28 ± 0.05) kJ·mol^{-1}. At the same time, in this sequence heat capacities of the crystal phases in the range of temperatures of (220 to 250) K decrease (Figure 9). Overall enthalpy increments for the transition from the crystal at $T =$ 200 K to the liquid at T_{fus}:

$$H_m^o(\text{liq};\ T_{fus}) - H_m^o(\text{cr};\ 200\ \text{K}) = \int_{200}^{T_{fus}} C_{p,m}(\text{cr})\,dT + \Delta_{fus}H_m^o \quad (9)$$

coincide within experimental error for all the crystals (Table 5).

The fusion temperatures for all the crystal phases and mole fraction of the main component in the samples under study were determined by the fractional-melting technique. The results are presented in Table 6. The experimental points are fitted by the van't Hoff equation:

$$T = T_0 - \left\{ \frac{RT_0^2}{\Delta_{fus}H_m^o} \cdot (1 - x) \right\} \cdot \frac{1}{f} \qquad (10)$$

where T_0 is a triple-point temperature in K; x is a mole fraction of the main component in a sample; $\Delta_{fus}H_m^o$ is an enthalpy of fusion; f is an equilibrium fraction of melt at temperature T. f is equal to the energy already expended to the fusion of the sample divided by $\Delta_{fus}H_m^o$.

The triple-point temperatures found from experiments with the different crystal phases and samples coincide within 0.01 K (Table 6 and Figure 15). The values

$$T_0 = (272.03 \pm 0.01)\ \text{K}, \quad x = (0.9976 \pm 0.0001)$$

were calculated from two series of fractional melting experiments for sample 1.

Similar joint treatment of the fractional-melting experiments for the different crystal phases of sample 2 lead to

$$T_0 = (272.03 \pm 0.01)\ \text{K}, \quad x = (0.9942 \pm 0.0001)$$

Amount of impurities in sample 2 is about 2.5 times higher than that in sample 1. This is probably due to the higher residual humidity of the second sample. If one assumes that water is the main impurity then the mass fraction of water in the samples is < 0.01 % for sample 1 and 0.02 % for sample 2.

Higher amount of impurities in the second sample has no measurable effect on the heat capacity of the β crystal and the liquid (Figure 10, Table 2), the fusion enthalpy of the β crystal (Table 4), and the triple-point temperature of the substance (Figure 15, Table 6).

Thermodynamic Functions. The smoothed values of heat capacities and thermodynamic functions of $[C_6mim][NTf_2]$ are presented in Table 7 for the glass and supercooled liquid states and in Table 8 for the crystal and liquid states. It was assumed in the calculations that differences in heat capacities of the crystal phases are negligible below 200 K, and at this temperature thermodynamic functions have the same values for all the crystals. Above 200 K a smoothing procedure and calculation of thermodynamic functions were applied separately for every crystal phase (Table 8).

In the low-temperature range (T < 10 K) one may neglect the difference between $C_{s,m}$ and $C_{v,m}$. A sum of Debye (D) and Einstein (E) contributions having 3 degrees of freedom each was used to extrapolate heat capacity of the substance below 5 K:

$$C_{s,m} \approx C_{v,m} = 3RD(\Theta_D/T) + 3RE(\Theta_E/T) \qquad (11)$$

The values of characteristic temperatures $\Theta_D = 48.5$ K and $\Theta_E = 43.5$ K for the crystal and $\Theta_D = 41.2$ K and $\Theta_E = 49.4$ K for the glass were obtained by the least-squares fitting of the experimental heat capacities in the ranges of temperatures (5.1 to 8.6) K and (5.2 to 8.4) K, respectively. In these temperature ranges, rms deviation of the experimental heat capacities from the ones calculated from eq 11 is < 1 %.

Thermodynamic properties of the liquid are calculated in reference to the α crystal (Table 8). Standard thermodynamic functions of liquid $[C_6mim][NTf_2]$ at $T = 298.15$ K are equal to

$$C_{p,m} = (629.2 \pm 2.5)\ \text{J·K}^{-1}\text{·mol}^{-1},$$
$$\Delta_0^T S_m^o = (755.8 \pm 3.2)\ \text{J·K}^{-1}\text{·mol}^{-1},$$
$$\Delta_0^T H_m^o/T = (405.1 \pm 1.8)\ \text{J·K}^{-1}\text{·mol}^{-1},$$
$$\Phi_m^o = (350.7 \pm 3.7)\ \text{J·K}^{-1}\text{·mol}^{-1}$$

Acknowledgment

The authors deeply appreciate Dr. J. Magee for initiation and continuous support of this work and Dr. M. Muldoon for the synethsis of $[C_6mim][NTf_2]$.

Supporting Information Available:

Three additional tables. This material is available free of charge via the Internet at http://pubs.acs.org.

Literature Cited

(1) Wasserscheid, P., Welton, T., Eds. *Ionic Liquids in Synthesis*; Wiley: New York, 2002; 364 pp.
(2) Paulechka, Y. U.; Kabo, G. J.; Lozinskaya, E. I.; Shaplov, A. S.; Vygodskii, Ya. S. Thermodynamics of 1-alkyl-3-methylimidazolium bromides. *Book of Abstracts, 1st International Congress on Ionic Liquids*, Salzburg, Austria, June 19−22, 2005; p 115.
(3) Kabo, G. J.; Blokhin, A. V.; Paulechka, Y. U.; Kabo, A. G.; Shymanovich, M. P.; Magee, J. W. Thermodynamic properties of 1-butyl-3-methylimidazolium hexafluorophosphate in the condensed state. *J. Chem. Eng. Data* **2004**, *49*, 453−461.
(4) Thermodynamics of ionic liquids, ionic liquid mixtures, and the development of standardized systems. IUPAC Project 2002-005-1-100; http://www.iupac.org/projects/2002/2002-005-1-100.html.
(5) http://www.termis.msk.ru/.
(6) Pavese, F.; Malyshev, V. M. Routine measurements of specific heat capacity and thermal conductivity of high-T_c superconducting materials in the range 4−300 K using modular equipment. *Adv. Cryog. Eng.* **1994**, *40*, 119−124.
(7) Varushchenko, R. M.; Druzhinina, A. I.; Sorkin E. L. Low-temperature heat capacity of 1-bromoperfluorooctane *J. Chem. Thermodyn.* **1997**, *29*, 623−637.
(8) Sabbah, R.; Xu-wu, A.; Chickos, J. S.; Planas Leitao, M. L.; Roux, M. V.; Torres, L. A. Reference materials for calorimetry and differential thermal analysis. *Thermochim. Acta* **1999**, *331*, 93−204.
(9) White, G. K.; Collocott, S. J. Heat capacity of reference materials: Cu and W. *J. Phys. Chem. Ref. Data* **1984**, *13*, 1251−1257.
(10) Rybkin, N. P.; Orlova, M. P.; Baranyuk, A. K.; Nurallaev, N. G.; Rozhnovskaya, L. N. Precise calorimetry at low temperatures. *Izmeritel. Tekh.* **1974**, *7*, 29−32 (in Russian).
(11) Ditmars, D. A.; Ishihara, S.; Chang, S. S.; Bernstein, G. Enthalpy and heat-capacity of standard reference material: synthetic sapphire (α-Al_2O_3) from 10 to 2250 K. *J. Res. Natl. Bur. Stand.* **1982**, *87*, 159−163.
(12) Furukawa, G. T.; Douglas, T. B.; McCoskey, R. E.; Ginning, D. C. Thermal properties of aluminium oxide from 0 to 1200 K. *J. Res. Natl. Bur. Stand.* **1956**, *57*, 67−82.
(13) Andrews, J. T. S.; Norton, P. A.; Westrum, E. F., Jr. An adibatic calorimeter for use at superambient temperatures. The heat capacity of synthetic supphire (α-Al_2O_3) from 300 to 550 K. *J. Chem. Thermodyn.* **1978**, *10*, 949−958.
(14) Stevens, R.; Boerio-Coates, J. Heat capacity of copper on the ITS-90 temperature scale using adiabatic calorimetry. *J. Chem. Thermodyn.* **2004**, *36*, 857−863.
(15) Kobashi, K.; Kyomen, T.; Oguni, M. Construction of an adiabatic calorimeter in the temperature range between 13 and 505 K, and thermodynamic study of 1-chloroadamantane. *J. Phys. Chem. Solids* **1998**, *59*, 667−677.
(16) Tatsumi, M.; Matsuo, T.; Suga, H.; Seki, S. An adiabatic calorimeter for high-resolution heat capacity measurements in the temperature range from 12 to 300 K. *Bull. Chem. Soc. Jpn.* **1975**, *48*, 3060−3066.

Received for review March 2, 2006. Accepted May 30, 2006. This work was performed as part of IACT/IUPAC Project 2002-005-1-100 "Thermodynamics of Ionic Liquids, Ionic Liquid Mixtures, and the Development of Standardized Systems" (coordinator Prof. K. Marsh) and with financial support of INTAS-Belarus foundation (Grant 03-50-5526, coordinator Prof. A. Heintz).

JE060094D